

Journal of Materials Chemistry C

Accepted Manuscript



This is an *Accepted Manuscript*, which has been through the Royal Society of Chemistry peer review process and has been accepted for publication.

Accepted Manuscripts are published online shortly after acceptance, before technical editing, formatting and proof reading. Using this free service, authors can make their results available to the community, in citable form, before we publish the edited article. We will replace this *Accepted Manuscript* with the edited and formatted *Advance Article* as soon as it is available.

You can find more information about *Accepted Manuscripts* in the [Information for Authors](#).

Please note that technical editing may introduce minor changes to the text and/or graphics, which may alter content. The journal's standard [Terms & Conditions](#) and the [Ethical guidelines](#) still apply. In no event shall the Royal Society of Chemistry be held responsible for any errors or omissions in this *Accepted Manuscript* or any consequences arising from the use of any information it contains.

Naphthodithiophenediimide (NDTI)-based triads for high-performance air-stable, solution-processed ambipolar organic field-effect transistors

Cite this: DOI: 10.1039/x0xx00000x

Received 00th January 2012,
Accepted 00th January 2012

Jian-Yong Hu,*^a Masahiro Nakano,^a Itaru Osaka^a and Kazuo Takimiya*^a

DOI: 10.1039/x0xx00000x

www.rsc.org/

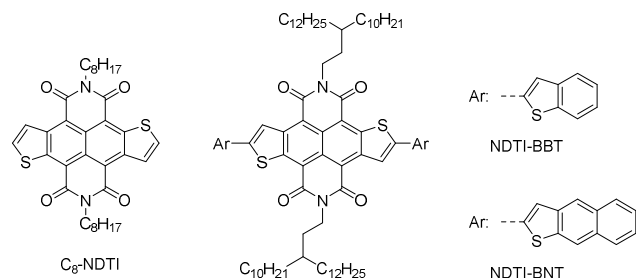
Two new NDTI-based triad-type ambipolar molecular semiconductors (NDTI-BBT and NDTI-BNT) were designed and synthesized. The triads can afford solution-processed OFETs with well-balanced, high hole and electron mobilities, up to 0.25 and 0.16 cm² V⁻¹s⁻¹, respectively, which further leads to a successful demonstration of complementary-like inverters with high voltage gains of 281 and 254 in the first and third quadrants, respectively, under the ambient conductions.

Ambipolar organic field-effect transistors (OFETs), using organic π -conjugated molecules¹ (such as squarylium dyes,^{1a,d} indigos,^{1e} isoindigos,^{1f} etc.) and polymers² (such as benzo(bis)thiadiazole-,^{2c} perylene diimide-,^{2d} diketopyrrolopyrrole-^{2e} based polymers) as active materials, have been attracting interest, because of their potential technological applications in complementary-like inverters³ and in light-emitting transistors.⁴ Especially, solution-processed ambipolar OFETs are expected to play a central role in large-area, low-cost, and flexible electronic devices. In view of molecular design for ambipolar organic semiconductors, two factors should be taken into account: 1) modifying the molecular structure to tune both the HOMO and LUMO energy levels for efficient hole and electron injection, respectively and to lower the reorganization energies to enhance carrier mobilities, and 2) controlling the molecular orientation and packing structure in the thin film state to facilitate large orbital overlap for better carrier transport. Accordingly, covalently linked donor-acceptor (D-A) conjugated molecules^{1b,5} and polymers⁶ have been reported as a single-component active material in ambipolar OFETs, where their HOMO and LUMO energy levels can be tuned by choosing suitable D and A units. However, “air-stable” ambipolar organic semiconductors capable of affording decent transistor characteristics for both p- and n-channel operations under the ambient conditions are still limited, and therefore development of such materials remains a challenge.

Naphthalene diimide (NDI), a representative electron-deficient π -unit with thermal and photochemical stability, and strong π -stacking behavior in the solid-state,⁷ has been used as a chromophore, an electronic material, and a supramolecular architecture.⁸ In recent years, the molecular modifications on NDI to produce NDI-based

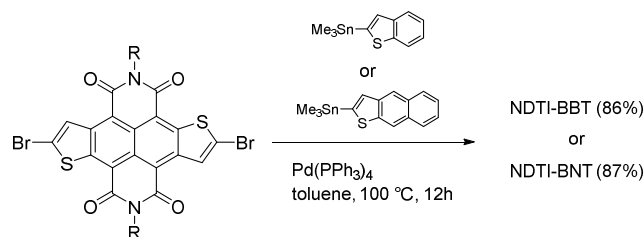
core-extended molecules⁹ and D-A polymers¹⁰ have been quite successful in developing p-type, n-type, and ambipolar organic semiconductors showing high mobilities. These prominent examples of the NDI-based materials have prompted us to develop a new versatile NDI-based core structure, a thiophene-fused NDI, namely, naphtho[2,3-*b*:6,7-*b'*]dithiophene-4,5,9,10-diimide (NDTI). In fact, we have demonstrated that NDTI is a useful electron-deficient building block for the development of n-type, p-type, and ambipolar organic semiconductors.¹¹

In this study, we have designed new NDTI-based conjugated triads, **NDTI-BBT** and **NDTI-BNT** (Scheme 1), potentially applicable to solution-processed ambipolar OFETs, where benzo[*b*]thiophene (BT) or naphtho[2,3-*b*]thiophene (NT) units are introduced at the thiophene α -positions to tune the HOMO energy level suitable for hole injection and large branched alkyl groups of 3-decylpentadecyl (DP) on the nitrogen atoms to ensure the solubility in organic solvents. Density functional theory (DFT) calculations on the triads, where the branched alkyl groups are substituted by methyl groups, using B3LYP functional and polarized 6-31g* basis set,¹² indicate that the HOMO energy levels of the triads are efficiently raised to 5.63 and 5.45 eV below the vacuum level for **NDTI-BBT** and **NDTI-BNT**, respectively, whereas the LUMO energy levels, 3.43 and 3.47 eV below the vacuum level, respectively, are almost identical with that of NDTI (calculated HOMO and LUMO energy levels are 6.05 and 3.47 eV, respectively, below the vacuum level, see also Table S1).¹¹ These calculations strongly suggest that the triads are expected to have suitable electronic structures for air-stable, ambipolar organic semiconductors. Furthermore, internal reorganization energies for the hole (λ^h , 204 and 112 meV for **NDTI-BBT** and **NDTI-BNT**, respectively) and electron transfer (λ^e , 161 and 165 meV for **NDTI-BBT** and **NDTI-BNT**, respectively), calculated from the adiabatic potential surfaces, are relatively small (see Table S1), indicating that the OFETs based on the triads could show high mobilities for both hole and electron. We here report on the synthesis, characterizations, and ambipolar natures of the NDTI-based triads. The characteristic feature of these triads is that they can afford balanced high hole and electron mobilities, up to 0.25 and 0.16 cm² V⁻¹s⁻¹, respectively, under the ambient conditions, which further enables us to fabricate air-stable complementary-like inverters with high voltage gains.



Scheme 1 Chemical structures of **C₈-NDTI**, **NDTI-BBT**, and **NDTI-BNT**.

The synthesis of the triads is outlined in Scheme 2, where *N,N'*-dialkyl-2,7-dibromo-NDTI¹¹ was reacted with 2-(trimethylstannyl)-benzo[*b*]thiophene or 2-(trimethylstannyl)naphtho[2,3-*b*]thiophene in the presence of the palladium catalyst to afford the target triads in high yields as dark-red solids. The triads were fully characterized by means of ¹H / ¹³C NMR spectra, mass spectroscopy, elemental analysis, and differential scanning calorimetry (DCS) (see Supporting Information). The triads have good solubility in common organic solvents, such as chloroform, toluene, and *o*-dichlorobenzene, which allowed us to fabricate OFET devices by using solution-deposition methods.



Scheme 2 Synthesis of **NDTI-BBT** and **NDTI-BNT**.

Fig. 1 shows the UV-vis absorption spectra of **NDTI-BBT** and **NDTI-BNT** recorded in chloroform solution and thin film state. Compared to the spectrum of **C₈-NDTI** in solution (λ_{max} : 554 nm),¹¹ clear bathochromic shifts caused by introducing the two BT or NT units are observed. The longest λ_{max} of the triad is 616 and 637 nm for the BT and NT triads, indicative of effective extension of the π -conjugation system. The absorption spectra of their thin films spun from the solution are markedly red-shifted compared to the solution spectra, possibly due to J-aggregate-like interactions in the thin film state.¹³ Note that the absorption band of the NT triad thin film largely red-shifts than the BT triad does, implying more effective intermolecular interactions for the former. The optical energy gaps estimated from the absorption onsets in the solution are *ca.* 1.86 and 1.76 eV for **NDTI-BBT** and **NDTI-BNT**, respectively. Cyclic voltammetry (CV) demonstrated that the triads are amphoteric within the typical electrochemical window (−1.1 ~ +1.5 V vs Fc/Fc⁺). From the onsets of oxidation and reduction waves, the HOMO and LUMO energy levels were estimated to be *ca.* −5.9 and −5.8 eV and −4.1 and −4.2 eV for **NDTI-BBT** and **NDTI-BNT**, respectively (Fig. S2 and Table S2). The electrochemical HOMO-LUMO gaps are well consistent with those estimated from the solution absorption spectra.

These physicochemical evaluation clearly indicate that the combination of the BT or NT with the NDTI unit effectively shifts the HOMO level upwards compared to that of **C₈-NDTI** (−6.1 eV) with keeping low-lying LUMO energy level.¹¹ As a result, the present triads, in particular **NDTI-BNT**, have ideal energy levels of HOMO and LUMO for the hole and electron transport under the ambient conditions.

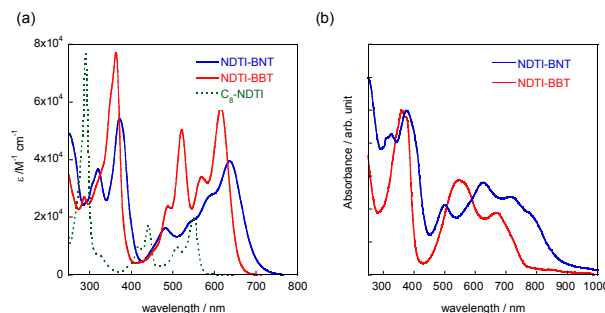


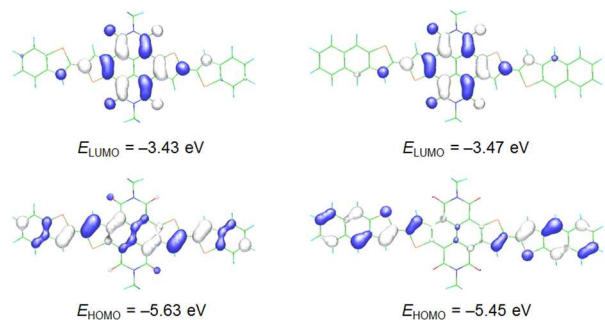
Fig. 1 UV-vis absorption spectra of **NDTI-BBT** and **NDTI-BNT**: (a) in chloroform solution and (b) in thin film.

Comparison between the empirical HOMO and LUMO energy levels and those estimated from the DFT calculations¹² can afford insights into the electronic structures of the triads. As already mentioned, the DFT calculations predicted that the introduction of the BT or NT on the NDTI unit can largely elevate the HOMO energy levels by more than 0.4 eV. However, this is not the case for the experimentally determined HOMOs; the upward shift from **C₈-NDTI** is only 0.2 or 0.3 eV for **NDTI-BBT** or **NDTI-BNT**, respectively. On the other hand, the electrochemically-determined LUMO energy levels for **C₈-NDTI**, **NDTI-BBT**, and **NDTI-BNT** are almost the same, which is consistent with the calculations. These inconsistent trends could be explained by taking into account the molecular structures and the geometries of HOMO and LUMO (Fig. 2). The DFT-optimized molecular structures of the triads are almost co-planar with the dihedral angles of $\sim 0^\circ$ (Fig. S4), and the HOMO coefficients are mostly on the lateral conjugation path through the two BT/NT and NDTI units. In the solution electrochemical measurements, the co-planarity between the π -units connected via single bonds can not be guaranteed, and the electrochemical HOMO energy levels could be underestimated. In contrast, the LUMOs of the triads are mainly contributed by the NDTI unit, which strongly implies that introduction of substituents and/or the co-planarity between them can make marginal perturbation to the LUMO energy levels of the present NDTI-based compounds. In addition, a marked difference in the calculated geometry of the HOMOs of **NDTI-BBT** and **NDTI-BNT** is noticed; for the former, the HOMO is delocalized over the whole triads, whereas the HOMO of the latter is much localized on the attached NT units, implying that efficiency of the orbital overlap of HOMOs in the solid state can be different, possibly affecting their hole transport properties.

Table 1 FET characteristics^a of **NDTI-BBT**- and **NDTI-BNT**-based devices with annealed thin films at different temperatures.

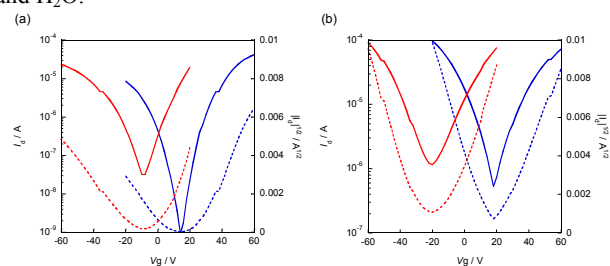
Compound	T_{anneal} [°C]	p-channel operation			n-channel operation		
		$\mu_{h, \text{max}}^b$ [cm ² V ⁻¹ s ⁻¹]	$I_{\text{on}}/I_{\text{off}}$	V_{th} [V]	$\mu_{e, \text{max}}^b$ [cm ² V ⁻¹ s ⁻¹]	$I_{\text{on}}/I_{\text{off}}$	V_{th} [V]
NDTI-BBT	as-spun	0.033 (0.031)	1.6×10^5	-22	0.042 (0.039)	2.4×10^4	29
	100	0.035 (0.032)	1.7×10^4	-20	0.043 (0.036)	4.5×10^3	31
	150	0.040 (0.036)	7.2×10^2	-17	0.17 (0.14)	4.5×10^2	33
	200	0.024 (0.020)	6.8×10^2	-19	0.077 (0.073)	3.6×10^4	30
NDTI-BNT	as-spun	0.044 (0.041)	5.3×10^2	-21	0.045 (0.040)	5.1×10^2	21
	100	0.071 (0.067)	2.0×10^2	-22	0.085 (0.076)	5.5×10^2	22
	150	0.25 (0.24)	79	-26	0.16 (0.14)	1.4×10^2	22
	200	0.14 (0.13)	1.1×10^2	-26	0.16 (0.15)	1.8×10^2	23

^a The p- and n-channel characteristics of ambipolar TFTs ($L = 40 \mu\text{m}$ and $W = 1500 \mu\text{m}$) were evaluated under the ambient conditions. ^b The mobility were extracted from the saturation regimes ($V_d = -60$ and $+60$ V for the p- and n-channel operations, respectively). The values in the parentheses are averaged mobilities from more than ten devices.

**Fig. 2** Calculated frontier orbitals of **NDTI-BBT** (left) and **NDTI-BNT** (right) by DFT/B3LYP-6-31g* level. The branched alkyl groups on the nitrogen atoms are substituted by methyl groups.

Thanks to their good solubilities, thin-film transistors of the triads were readily fabricated by spin-coating of their solution onto the octadecyltrichlorosilane (ODTS)-treated Si/SiO₂ substrate followed by vacuum deposition of the gold source and drain electrodes, resulting in the devices with the bottom-gate-top-contact (BGTC) configuration. As expected from the HOMO and LUMO energy levels, the devices showed typical ambipolar characteristics under the ambient conditions (Table 1). Hole and electron mobilities of the devices with as-spun thin films extracted from the saturation regime are moderately high and well balanced, 0.033 and 0.042 cm² V⁻¹ s⁻¹ for the **NDTI-BBT**- and 0.044 and 0.045 cm² V⁻¹ s⁻¹ for the **NDTI-BNT**-based devices, respectively. Thermal annealing of the thin films can effectively improve the mobilities of the triad-based devices (Table 1), which can be ascribed to the improved crystalline ordering of molecules in the thin film state (vide infra). The maximum hole/electron mobilities are 0.040/0.17 cm² V⁻¹ s⁻¹ for the **NDTI-BBT**- and 0.25/0.16 cm² V⁻¹ s⁻¹ for the **NDTI-BNT**-based devices with the thin films annealed at 150 °C for 30 minutes (Fig. 3). It should be pointed out that the present electron mobilities are higher than that of C₈-**NDTI**-based OFETs (up to 0.055 cm² V⁻¹ s⁻¹),^{11a} and the hole mobility of **NDTI-BNT** is comparable to that of the NT-dimer, [2,2']bi[naphtho[2,3-*b*]thiophenyl], (up to 0.67 cm² V⁻¹ s⁻¹),¹⁴ indicating that the current triad approach is effective to develop well-performing ambipolar organic semiconductors. It is noteworthy that slight decreased hole/electron mobilities are measured for **NDTI-BBT**- and **NDTI-BNT**-based OFETs in a 150 °C-annealed film even after 1 week of storage in air (20–40% humidity) (Fig. S9 and Table S3), indicating

negligible deterioration due to atmospheric oxidants¹⁵ such as O₂ and H₂O.

**Fig. 3** Transfer characteristics of **NDTI-BBT**- (a) and **NDTI-BNT**- (b) based transistors evaluated under the ambient conditions (annealed at 150 °C).

In the out-of-plane XRDs of the as-spun **NDTI-BBT** thin film, two series of lamellar peaks were observed, corresponding to coexistence of different packing motifs. Thermal annealing, however, drastically improved the uniformity and crystallinity of the film,^{9k} as evidenced by the observation of only one series of peaks assigned to the lamella structure with a d -spacing of ca. 35 Å (Fig. 4a). On the other hand, the as-spun **NDTI-BNT** thin film showing broad and less intensive peaks in the out-of-plane XRD became highly crystalline with the lamella ordering with a d -spacing of ca. 33 Å upon thermal annealing (Fig. 4b). In addition to the obvious lamella ordering in the out-of-plane XRDs, the in-plane XRDs of the both thin films showed clear peaks at around $2\theta = 26^\circ$, which might be assignable to π - π stacking (ca. 3.5 Å, Fig. 4c). From these thin film XRD patterns, it can be concluded that both compounds have a similar packing structure in the thin film state, where the molecules stand on the substrate surface with π -stacking arrays in the lateral direction.¹⁶

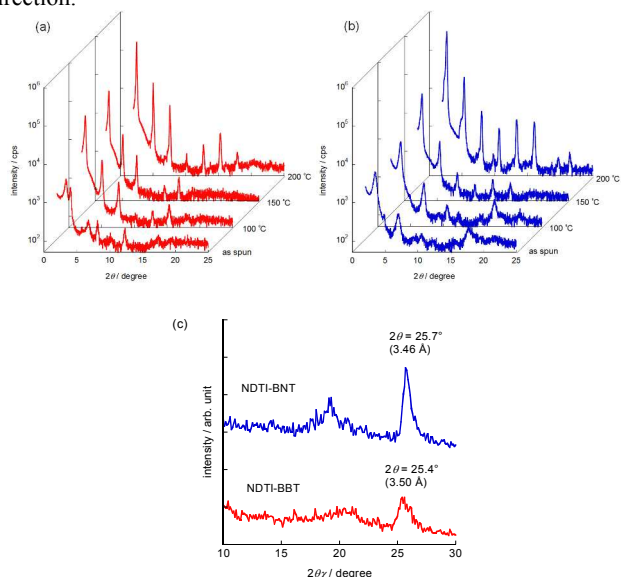


Fig. 4 Out-of-plane XRD patterns of **NDTI-BBT**- (a) and **NDTI-BNT**-thin films (b) annealed at different temperatures, and in-plane XRD patterns of **NDTI-BBT**- and **NDTI-BNT**-thin films (c) annealed at 150 °C.

It is interesting to point out that the hole mobility is only enhanced for the **NDTI-BNT**-based devices up to $0.25 \text{ cm}^2 \text{ V}^{-1} \text{ s}^{-1}$, whereas the electron mobilities for both compounds are almost the same ($\sim 0.17 \text{ cm}^2 \text{ V}^{-1} \text{ s}^{-1}$). This can be explained by the molecular and electronic structures of two compounds; as discussed already, the HOMO of the triads tends to reside in the lateral conjugation path consisting of the two BT/NT units through the NDTI unit, whereas the LUMO tends to localize on the central NDTI unit (Fig. 2). In the annealed thin films with improved crystallinity, in which both compounds are supposed to have a similar packing structure, intermolecular orbital overlaps could be significantly affected by the geometry and/or extensity of molecular orbitals. For the better intermolecular orbital overlap of HOMOs, **NDTI-BNT** with the extended HOMO on two NT units should be more advantageous than **NDTI-BBT**, whereas the localized LUMO on the NDTI unit for both compounds can result in a similar efficiency of the

intermolecular LUMO-LUMO overlap. From these consideration based on the experimental results along with the theoretical calculations, we can conclude that extension of π -conjugation in the lateral direction, *i.e.*, the direction of naphtho[2,3-*b*:6,7-*b'*]dithiophene in the NDTI unit, which inherently has the low-lying LUMO ($\sim -4.0 \text{ eV}$), should be a rational molecular design strategy for air-stable ambipolar organic semiconductor with well-balanced high hole and electron mobilities.^{7a}

To further demonstrate the advantages of **NDTI-BNT** capable of affording well-balanced high hole and electron mobilities, we also fabricated complementary-like inverters on single substrates using two identical transistors with the shared gold gate. Fig. 5 shows the voltage transfer characteristics of the inverter annealed at 150 °C, operated at a supplied voltage (V_{DD}) of +60 and -60 V under the ambient conditions. The inverter exhibited a sharp switching of V_{out} , both in the first and third quadrants with the voltage gains of 281 and 254, respectively.

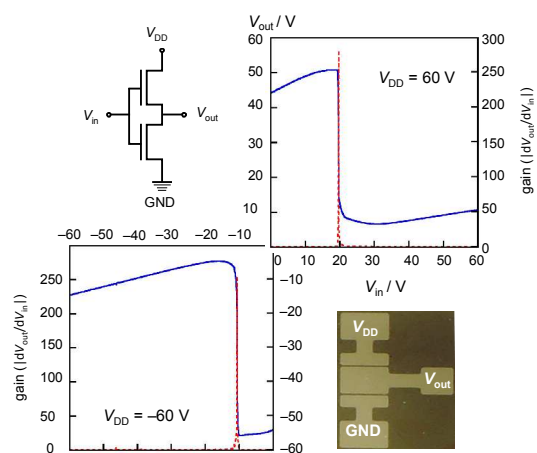


Fig. 5 Voltage transfer characteristics of a complementary inverter consisting of two identical **NDTI-BNT**-based ambipolar transistors with supplied voltage of +60 and -60 V. Insets show a circuit diagram and a photograph of the device.

In summary, we have successfully demonstrated that a rational molecular design by using the NDTI unit can produce air-stable, solution-processable, ambipolar molecular semiconductors that afford reasonably high and balanced hole and electron mobilities. It should be emphasized that the present NDTI-based triads are rare examples of non-polymer materials capable of affording decent solution-processed ambipolar transistors operable under the ambient conditions. In addition to these electrical properties, the present molecular design for ambipolar semiconductors, which can be regarded as combination of different functional moieties without disturbing other functionality, seems to be rational. In the NDTI-based triads, the ability of NDTI as the electron transport moiety is well preserved even after introduction of the BT or NT moieties as the hole transport part. In addition, the branched alkyl groups, affording the solubilizing nature to the materials, do not disturb the efficient intermolecular orbital overlap through the π - π stacking structure, probably owing to their placement slightly apart from the π -conjugation core of the triads. We believe that this kind of concept can also be applicable to other π -functional moieties¹⁷ for

developing ambipolar molecular semiconductors, not relying too much on the prevailing D-A alternating conjugated polymers, and hope that further superior ambipolar molecules will be developed in near future.

Acknowledgements

This work was financially supported by Grants-in-Aid for Scientific Research (Nos. 23245041 and 26810109) from MEXT, Japan. The DFT calculations were performed by using the RIKEN Integrated Cluster of Clusters (RICC). One of the authors (M.N.) is grateful for the Postdoctoral Fellowship of Japan Society for the Promotion of Science (JSPS).

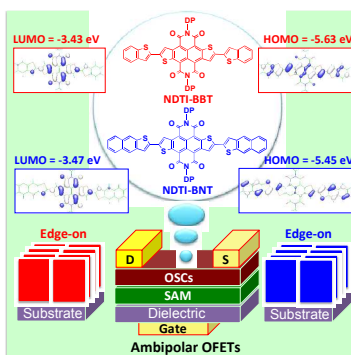
Notes and references

^a Emergent Molecular Function Research Group, RIKEN Center for Emergent Matter Science (CEMS), Wako, Saitama 351-0198, Japan E-mail: jian-yong.hu@riken.jp; takimiya@riken.jp.

† Electronic Supplementary Information (ESI) available: Synthetic details, additional device characterization data. See DOI: 10.1039/c000000x/

- (a) E. C. P. Smits, S. Setayesh, T. D. Anthopoulos, M. Buechel, W. Nijssen, R. Coehoorn, P. W. M. Blom, B. de Boer and D. M. de Leeuw, *Adv. Mater.*, 2007, **19**, 734; (b) A. R. Murphy and J. M. Frechet, *Chem. Rev.*, 2007, **107**, 1066; (c) M. Mas-Torrent and C. Rovira, *Chem. Soc. Rev.* 2008, **37**, 827; (d) P. H. Wöbkenberg, J. G. Labram, J.-M. Swiecicki, K. Parkhomenko, D. Sredojevic, J.-P. Gisselbrecht, D. M. de Leeuw, D. D. C. Bradley, J.-P. Djukic and T. D. Anthopoulos, *J. Mater. Chem.* 2010, **20**, 3673; (e) E. D. Głowacki, G. Voss and N. S. Sariciftci, *Adv. Mater.*, 2013, **25**, 6783; (f) E. Wang, W. Mammo and M. R. Andersson, *Adv. Mater.*, 2014, **26**, 1801.
- (a) J. Zaumseil and H. Sirringhaus, *Chem. Rev.*, 2007, **107**, 1296; (b) A. Facchetti, *Chem. Mater.* 2011, **23**, 733; (c) T. Dallos, D. Beckmann, G. Brunklaus and M. Baumgarten, *J. Am. Chem. Soc.*, 2011, **133**, 13898; (d) H. Usta, C. Newman, Z. Chen and A. Facchetti, *Adv. Mater.*, 2012, **24**, 3678; (e) J. Lee, A.-R. Han, J. Kim, Y. Kim, J. H. Oh and C. Yang, *J. Am. Chem. Soc.*, 2012, **134**, 20713.
- (a) E. J. Meijer, D. M. De Leeuw, S. Setayesh, E. Van Veenendaal, B.-H. Huisman, P. W. Blom, J. C. Hummelen, U. Scherf and T. M. Klapwijk, *Nat. Mater.*, 2003, **2**, 678; (b) J. C. Bijleveld, A. P. Zoombelt, S. G. J. Mathijssen, M. M. Wienk, M. Turbiez, D. M. de Leeuw and R. A. J. Janssen, *J. Am. Chem. Soc.*, 2009, **131**, 16616; (c) F. S. Kim, X. Guo, M. D. Watson and S. A. Jenekhe, *Adv. Mater.*, 2010, **22**, 478; (d) J. Fan, J. D. Yuen, M. F. Wang, J. Seifter, J. H. Seo, A. R. Mohebbi, D. Zakhidov, A. Heeger and F. Wudl, *Adv. Mater.*, 2012, **24**, 2186; (e) K.-J. Baeg, D. Khim, S.-W. Jung, M. Kang, I.-K. You, D.-Y. Kim, A. Facchetti and Y.-Y. Noh, *Adv. Mater.*, 2012, **24**, 5433; (f) J. Lee, A.-R. Han, J. Kim, Y. Kim, J. H. Oh and C. Yang, *J. Am. Chem. Soc.*, 2012, **134**, 20713; (g) H.-J. Yun, H. H. Choi, S.-K. Kwon, Y.-H. Kim and K. Cho, *Chem. Mater.*, 2014, **26**, 3928.
- (a) J. Zaumseil, C. L. Donley, J. S. Kim, R. H. Friend and H. Sirringhaus, *Adv. Mater.*, 2006, **18**, 2708; (b) L. Bürgi, M. Turbiez, R. Pfeiffer, F. Bienewald, H.-J. Kirner and C. Winnewisser, *Adv. Mater.*, 2008, **20**, 2217; (c) S. N. Bhat, R. D. Pietro and H. Sirringhaus, *Chem. Mater.*, 2012, **24**, 4060; (d) M. C. Gwinner, D. Kabra, M. Roberts, T. J. K. Brenner, B. H. Wallikewitz, C. R. McNeill, R. H. Friend and H. Sirringhaus, *Adv. Mater.*, 2012, **24**, 2728.
- (a) R. J. Chesterfield, C. R. Newman, T. M. Pappenfus, P. C. Ewbank, M. H. Haukaas, K. R. Mann, L. L. Miller and C. D. Frisbie, *Adv. Mater.*, 2003, **15**, 1278; (b) L. E. Polander, L. Pandey, S. Barlow, S. P. Tiwari, C. Risko, B. Kippelen, J.-L. Brédas and S. R. Marder, *J. Phys. Chem. C.*, 2011, **115**, 23149; (c) W. Kang, M. Jung, W. Cha, S. Jang, Y. Yoon, H. Kim, H. J. Son, D.-K. Lee, B. Kim and J. H. Cho, *ACS Appl. Mater. Interfaces*, 2014, **6**, 6589; (d) Q. Shuai, H. T. Black, A. Dadvand and D. F. Perepichka, *J. Mater. Chem. C.*, 2014, **2**, 3972.
- (a) M. Muccini, *Nat. Mater.*, 2006, **5**, 605; (b) P. Sonar, S. P. Singh, Y. Li, M. S. Soh and A. Dodabalapur, *Adv. Mater.*, 2010, **22**, 5409; (c) K.-J. Baeg, M. Caironi and Y.-Y. Noh, *Adv. Mater.*, 2013, **25**, 4210; (d) J. Lee, A.-R. Han, H. Yu, T. J. Shin, C. Yang and J. H. Oh, *J. Am. Chem. Soc.*, 2013, **135**, 9540.
- (a) F. Würthner and M. Stolte, *Chem. Commun.*, 2011, **47**, 5109; (b) S.-L. Suraru and F. Würthner, *Angew. Chem. Int. Ed.*, 2014, **53**, 7428.
- (a) H. Vollmann, H. Becker, M. Corell and H. Streeck, *Lieb. Ann.*, 1937, **531**, 1; (b) S. V. Bhosale, C. H. Jani and S. J. Langford, *Chem. Soc. Rev.*, 2008, **37**, 331; (c) X. Zhan, A. Facchetti, S. Barlow, T. J. Marks, M. A. Ratner, M. R. Wasielewski and S. R. Marder, *Adv. Mater.*, 2011, **23**, 268.
- (a) H. E. Katz, A. J. Lovinger, J. Johnson, C. Kloc, T. Siegrist, W. Li, Y.-Y. Lin and A. Dodabalapur, *Nature*, 2000, **404**, 478; (b) X. Gao, C.-A. Di, Y. Hu, X. Yang, H. Fan, F. Zhang, Y. Liu, H. Li and D. Zhu, *J. Am. Chem. Soc.*, 2010, **132**, 207133697; (c) J. H. Oh, S.-L. Suraru, W.-Y. Lee, M. Könemann, H. W. Höffken, C. Röger, R. Schmidt, Y. Chung, W.-C. Chen, F. Würthner and Z. Bao, *Adv. Funct. Mater.*, 2010, **20**, 2148; (d) S.-L. Suraru, U. Zschieschang, H. Klauk and F. Würthner, *Chem. Commun.*, 2011, **47**, 11504; (e) Y. Hu, X. Gao, C.-A. Di, X. Yang, F. Zhang, Y. Liu, H. Li and D. Zhu, *Chem. Mater.* 2011, **23**, 1204; (f) Y. Zhao, C.-A. Di, X. Gao, Y. Hu, Y. Guo, L. Zhang, Y. Liu, J. Wang, W. Hu, D. Zhu, *Adv. Mater.* 2011, **23**, 2448; (g) L. Tan, Y. Guo, G. Zhang, Y. Yang, D. Zhang, G. Yu, W. Xu and Y. Liu, *J. Mater. Chem.*, 2011, **21**, 18042; (h) P. Deng, Y. Yan, S.-D. Wang and Q. Zhang, *Chem. Commun.*, 2012, **48**, 2591; (i) R. P. Ortiz, H. Herrera, C. Seoane, J. L. Segura, A. Facchetti and T. J. Marks, *Chem. Eur. J.*, 2012, **18**, 532; (j) Y. Hu, Y. Qin, X. Gao, F. Zhang, C.-A. Di, Z. Zhao, H. Li and D. Zhu, *Org. Lett.*, 2012, **14**, 292; (k) F. Zhang, Y. Hu, T. Schuettfort, C.-A. Di, X. Gao, C. R. McNeill, L. Thomsen, S. C. B. Mannsfeld, W. Yuan, H. Sirringhaus and D. Zhu, *J. Am. Chem. Soc.*, 2013, **135**, 2338; (l) C. Li, C. Xiao, Y. Li and Z. Wang, *Org. Lett.*, 2013, **15**, 682; (m) R. P. Ortiz, H. Herrera, M. J. Manchoño, C. Seoane, J. L. Segura, P. M. Burrezo, J. Casado, J. T. L. Navarrete, A. Facchetti and T. J. Marks, *Chem. Eur. J.*, 2013, **19**, 12458; (n) X. Gao and Y. Hu, *J. Mater. Chem. C.*, 2014, **2**, 3099.
- (a) H. Yan, Z. Chen, Y. Zheng, C. Newman, J. R. Quinn, F. Dötz, M. Kastler and A. Facchetti, *Nature*, 2009, **457**, 679; (b) J. Rivnay, M. F. Toney, Y. Zheng, I. V. Kauvar, Z. Chen, V. Wagner, A. Facchetti and A. Salleo, *Adv. Mater.*, 2010, **22**, 4359; (c) X. Guo, F. S. Kim, M. J. Seger, S. A. Jenekhe and M. D. Watson, *Chem. Mater.*, 2012,

- 24, 1434; (d) W. Zhou, Y. Wen, L. Ma, Y. Liu and X. Zhan, *Macromolecules*, 2012, **45**, 4115; (e) C. Gu, W. Hu, J. Yao and H. Fu, *Chem. Mater.*, 2013, **25**, 2178; (f) Y. Kim, J. Hong, J. H. Oh and C. Yang, *Chem. Mater.*, 2013, **25**, 3251; (g) H. Chen, Y. Guo, Z. Mao, G. Yu, J. Huang, Y. Zhao and Y. Liu, *Chem. Mater.*, 2013, **25**, 3589; (h) R. Steyrlleuthner, R. D. Pietro, B. A. Collins, F. Polzer, S. Himmelberger, M. Schubert, Z. Chen, S. Zhang, A. Salleo, H. Ade, A. Facchetti and D. Neher, *J. Am. Chem. Soc.*, 2014, **136**, 4245; (i) N. B. Kolhe, A. Z. Ashar, K. S. Narayan and S. K. Asha, *Macromolecules*, 2014, **47**, 2296.
- 11 (a) Y. Fukutomi, M. Nakano, J.-Y. Hu, I. Osaka and K. Takimiya, *J. Am. Chem. Soc.*, 2013, **135**, 11445; (b) E. Zhou, M. Nakano, S. Izawa, J. Cong, I. Osaka, K. Takimiya and K. Tajima, *ACS Macro Lett.* 2014, **3**, 872; (c) M. Nakano, I. Osaka and K. Takimiya, *Macromolecules* 2015, **48**, 576.
- 12 Gaussian 09, Revision C.01, M. J. Frisch, G. W. Trucks, H. B. Schlegel, G. E. Scuseria, M. A. Robb, J. R. Cheeseman, G. Scalmani, V. Barone, B. Mennucci, G. A. Petersson, H. Nakatsuji, M. Caricato, X. Li, H. P. Hratchian, A. F. Izmaylov, J. Bloino, G. Zheng, J. L. Sonnenberg, M. Hada, M. Ehara, K. Toyota, R. Fukuda, J. Hasegawa, M. Ishida, T. Nakajima, Y. Honda, O. Kitao, H. Nakai, T. Vreven, J. A. Montgomery, Jr., J. E. Peralta, F. Ogliaro, M. Bearpark, J. J. Heyd, E. Brothers, K. N. Kudin, V. N. Staroverov, R. Kobayashi, J. Normand, K. Raghavachari, A. Rendell, J. C. Burant, S. S. Iyengar, J. Tomasi, M. Cossi, N. Rega, J. M. Millam, M. Klene, J. E. Knox, J. B. Cross, V. Bakken, C. Adamo, J. Jaramillo, R. Gomperts, R. E. Stratmann, O. Yazyev, A. J. Austin, R. Cammi, C. Pomelli, J. W. Ochterski, R. L. Martin, K. Morokuma, V. G. Zakrzewski, G. A. Voth, P. Salvador, J. J. Dannenberg, S. Dapprich, A. D. Daniels, Ö. Farkas, J. B. Foresman, J. V. Ortiz, J. Cioslowski, and D. J. Fox, Gaussian, Inc., Wallingford CT, 2009.
- 13 A. Mishra, R. K. Behera, P. K. Behera, B. K. Mishra and G. B. Behera, *Chem. Rev.*, 2000, **100**, 1973.
- 14 M. Mamada, J.-i. Nishida, D. Kumaki, S. Tokito and Y. Yamashita, *J. Mater. Chem.*, 2008, **18**, 3442.
- 15 T. D. Anthopoulos, G. C. Anyfantis, G. C. Papavassiliou, D. M. de Leeuw, *Appl. Phys. Lett.*, 2007, **90**, 122105.
- 16 From the XRD patterns in Fig. 3a and Fig. 3b, it is obvious that the thin films of the triads annealed at 200 °C have better crystallinity than those annealed at 150 °C. However, their surface morphology revealed by AFM images demonstrated that uniformity of film reduces significantly in the 200 °C-annealed one with pronounced grain boundaries. See Fig. S11 and Fig. S12 in supporting information.
- 17 K. Takimiya, I. Osaka and M. Nakano, *Chem. Mater.*, 2014, **26**, 587.

Graphical Abstract:

New triad-type ambipolar molecular semiconductors have been developed by covalently integrating two benzo[b]thiophene (BT) or naphtho[2,3-b]thiophene (NT) units into the naphthodithiophenediimide (NDTI) building block. Their HOMO and LUMO lay at the ideal energy levels for air-stable hole/electron transports. In fact, in combination with their lamella packing structures with close π -stacking ordering in the thin film state, the triads can afford solution-processed OFETs with well-balanced, high hole and electron mobilities, up to 0.25 and 0.16 $\text{cm}^2 \text{V}^{-1} \text{s}^{-1}$, respectively, which further leads to a successful demonstration of complementary-like inverters with high gain under the ambient conditions.